Clinical Neurophysiology 155 (2023) 55–57

Contents lists available at ScienceDirect

Clinical Neurophysiology

journal homepage: www.elsevier.com/locate/clinph

Letter to the Editor

Multimodal invasive and noninvasive neuroimaging and SEEG analyses prior to surgical treatment of MRI-negative occipital lobe epilepsy

Occipital lobe epilepsy (OLE) is by far the least common epilepsy among the extratemporal epilepsy group and is often under-recognized or misdiagnosed to its variable electroclinical manifestation from extensive connectivity to extra-occipital cortices (Jobst et al., 2010). Consequently, invasive intracranial (icEEG) recordings are frequently required in OLE and often demonstrate extensive epileptogenic zones (EZ) (Heo et al., 2018; Jobst et al., 2010). Due to anatomical variation in the sulcal and gyral patterns of the occipital lobe, it is further challenging to detect subtle lesions on MRI (Alves et al., 2012). Standard pre-surgical noninvasive modalities such as ictal single photon emission computed tomography (SPECT), fluorodeoxyglucose positron emission tomography (FDG-PET), and magnetoencephalography (MEG) have been shown to guide that optimal icEEG coverage in MRI negative OLE to improve seizure freedom as well as the quality of life by preserving visual function (quadrantanopia vs. hemianopsia), although they can still be inconclusive (Heo et al., 2018; Jobst et al., 2010). Voxel-based morphometric (VBM) MRI post-processing and MRI co-registered FDG-PET offer an adjunct to other non-invasive presurgical evaluations in refining the optimal icEEG electrode placement (Chassoux et al., 2010; Huppertz et al., 2009). In addition, an EZ electrophysiologic biomarker, "EZ fingerprint," has been recently described using time–frequency analysis and validated in focal epilepsies (Grinenko et al., 2018). Here, we present an MRI-negative DR-OLE patient who underwent prospective application of the post-processing MRI and MRI co-registered FDG-PET leading to optimal stereo-encephalography (SEEG) electrode placement, complemented with post-processing of electrophysiological data using "EZ fingerprint" pipeline (Jian, 2018, 2020) to localize the EZ further.

Before the SEEG implantation, preoperative 3 T T1-weighed 1 mm isotropic Magnetization Prepared Rapid Acquisition with Gradient Echo (MPRAGE) images were acquired and post-processed using a morphometric analysis program (MAP) in Statistical Parametric Mapping (SPM; Wellcome Department of Cognitive Neurology, London, United Kingdom) within MATLAB 2022a (Math-Works, Natick, MA, U.S.A.) (Huppertz et al., 2005, 2009) The z-score of 4 was used to identify highlighted areas on the junction file (Huppertz et al., 2009, 2005). FDG-PET scan was overlaid on the MRI using SPM. SEEG electrode was adjusted according to the highlighted region detected with post-processing MAP and MRI-PET evaluations. EZ electrode contacts were predicted using the "EZ fingerprint" pipeline (Jian, 2018, 2020), where the support vector machine prediction model was trained using the patient data from our previous study (Grinenko et al., 2018).

The patient was a 34-year-old right-handed male with long-standing history (~21 years) of focal epilepsy, factor V Leiden mutation, and recurrent acute kidney injury. Seizure semiology was described as right visual field blurring (about 5–10% of the seizures) with the feeling of the eye pulling toward the right side lasting for 2–10 s, followed by right hemianopsia. If prolonged, he became amnestic to the event, followed by right face clonic and head deviation to the right side with secondary generalization. After failing seven antiseizure medications, he continued to have seizures once to twice per month. No interictal spikes, but the scalp ictal onset was noted as an intrusion of paroxysmal fast activity evolving over the left occipitotemporal region with diffuse bihemispheric involvement. MRI was unremarkable (Fig. 1A). FDG-PET scan showed overall diffuse subtle decreased metabolism over the left parieto-occipital regions. SPECT and MEG were unable to be performed. MRI post-processing analysis using MAP highlighted an area in the tip of the left lingula cortex ($z > 4$) corresponding to gray-white junction blurring (Fig. 1B) with corresponding localized hypometabolism of FDG-PET over MAP+ (Fig. 1C). SEEG monitoring was proposed to investigate the hypotheses of the left occipital lobe (lingula), parietal, and lateral posterior temporal region (Fig. 1D). With the post-processing data, electrode F' was planned to pass through the MAP+/MAP + PET region (Fig. 1E). Continuous spikes and polyspikes were noted only over mesial lingula F'1-3 (i.e., mesial to the margin of the MAP +) (Fig. 1E, F). A total of 21 stereotypical seizures were recorded. EEG onset was noted as the resolution of spike activity in left medial lingula gyrus (F' 1–3) with the intrusion of low voltage fast activity synchronous with left lateral occipital gyrus (O'13–15), fusiform gyrus (post: F' 6–9 contacts, ant: E'1–5) followed by involvement of fast activity in the lateral superior occipital gyrus (V'7-10), calcarine sulcus (D' 4–6) within a few milliseconds. Within one second, intrusion of fast activity was noted in the primary visual regions O' mesial was noted, and the patient reported right-sided upper quadrantanopia, showing adequate anatomo-functional-electro-clinical correlations of SEEG orthogonal latero-medial trajectory implantation (Fig. 1F and Fig. 2). The electrode stimulation of the mesial lingula cortex (F' 1–2) at 0.5 mA (50 Hz, 300 μsec pulse width and 4 s train) (Fig. 2) triggered a typical spontaneous seizure. The 21 seizures were analyzed through the "EZ Fingerprint"

Abbreviations: MEG, magnetoencephalography
EEG, electroencephalography
MRI, magnetic resonance imaging
OLE, occipital lobe epilepsy
SEEG, stereoelectroencephalography
SPECT, single photon emission computed tomography
FDG-PET, fluorodeoxyglucose positron emission tomography
EZ, epileptogenic zone
VBM, Voxel-Based Morphometry
SPM, statistical parametric mapping

https://doi.org/10.1016/j.clinph.2023.08.014

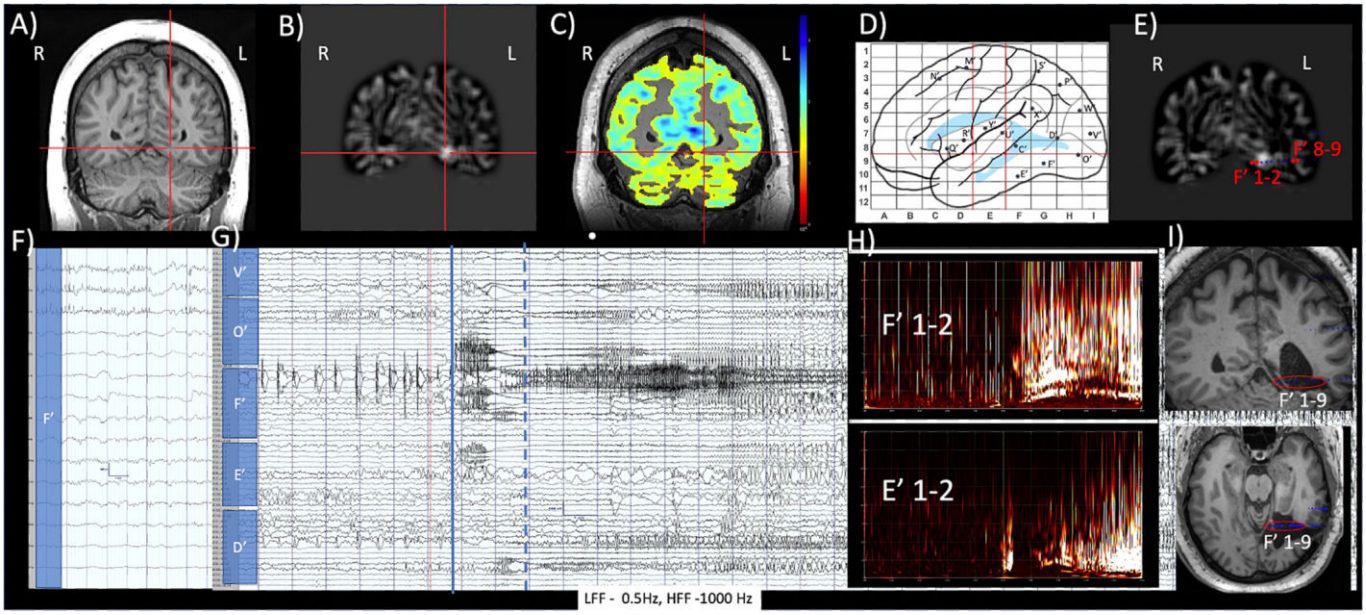

Fig. 1. A: Region of left lingula gyrus corresponding with MAP + regions, B: MAP + left lingula gyrus (z score of 6.8), C: Corresponding decreased glucose metabolism FDG-PET overlaid on the MRI using statistical parametric mapping (SPM, http://neuroimage.usc.edu/brainstorm), D: Electrode implantation trajectories and plan on the Talairach grid, E: F' SEEG electrode contact piercing through the voxel based morphometry lesion with the major interictal activity is noted in the mesial contacts (F'1-3), F: Interictal ictal transition with resolution of spike activity in left medial lingula gyrus (F' 1–3) with the intrusion of low voltage fast activity synchronous with left lateral occipital gyrus (O'13–15), fusiform gyrus (post: F' 6–9 contacts, ant: E'1–5) followed by involvement of fast activity in the lateral superior occipital gyrus (V'7-10), calcarine sulcus (D' 4–6) within a few milliseconds (red line). Within one second, intrusion of fast activity was noted in the primary visual regions- O' mesial electrodes (blue dotted line), with the patient reporting right side upper quadrantanopia. H: comparing normalized time–frequency pattern (between interictal and ictal 40 seconds) of predicted contact F' 1–2 (the pattern of preictal spiking, fast activity with corresponding suppression) and no predicted EZ contact E'1-2. I: Postsurgical MRI overlaid with the F' contact resulting in the resection of F' 1–9 contacts. Abbreviations: LFF, low-frequency filter; HFF, high-frequency filter.

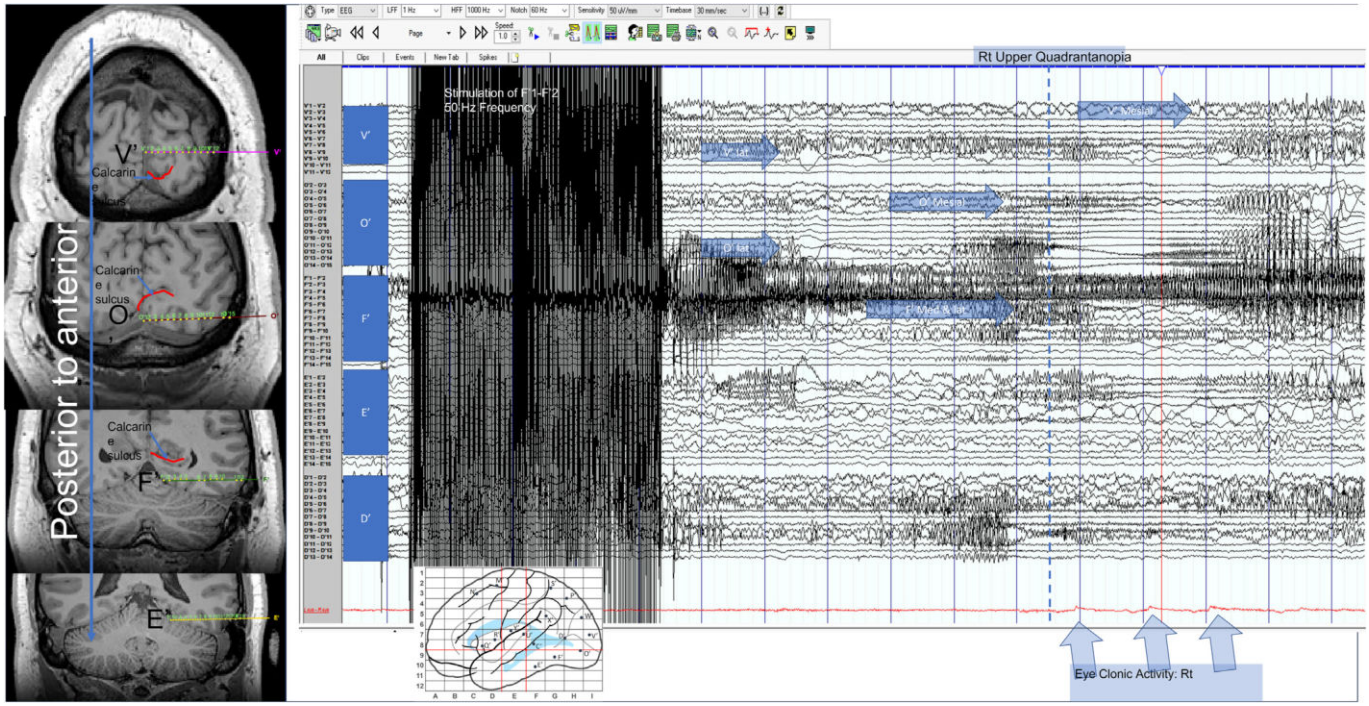

Fig. 2. Electrode location in relation to the perfect anatomo-functional-electro-clinical correlations of stereo-EEG orthogonal latero-medial trajectory implantation following the stimulation F' 1–2 contact at 50 Hz, 300 μs, 4 s train at 0.5 mA. The stimulation triggered the stereotypical ictal event. Right after the stimulation artifact, there was intrusion of synchronous polyspikes activity involving the left lateral occipital gyrus (O'13–15), fusiform gyrus (post: F' 6–9 contacts, ant: -E'1–5) followed by involvement of fast activity in the lateral superior occipital gyrus (V'7-10), calcarine sulcus (D' 4–6) within a few milliseconds. Within seconds, intrusion of fast activity was noted in the primary visual regions- O' mesial contacts, and the patient reported right side upper quadrantanopia (blue dotted line). After a few seconds, the patient reported right hemianopsia (redline) when the intrusion of fast activity was noted in V' mesial contact.

pipeline, where F'1-2 and F'3-4 were predicted to be within the EZ (Fig. 1H). The patient underwent resection of the lingula cortex (Fig. 1I), resulting in quadrantanopia. Pathology was unable to be analyzed due to the tissue being damaged, but the patient remained seizure-free for 41 months without language abnormality.

The case highlights the clinical challenges of OLE. MRI/MRI-PET post-processing can provide an important adjunct to the presurgical evaluation for optimal SEEG electrode placement, overcoming the limitation of intrinsic poor spatial limitation of SEEG. In this particular case, although interictal ictal SEEG transition (ictal onset) was fairly extensive with synchronous fast activities in the vast majority of the occipital lobe and the basal temporal regions, the optimal SEEG electrode trajectory (F' electrode) led to exploring the exact relationship of EZ, irritative zone, lesional zone, and symptomatogenic zone in OLE. The EZ electrophysiologic biomarker, the "EZ fingerprint" pattern is the complex pattern of the electrical biomarker EZ, including the combination of preceding spikes and multiband fast activity with concurrent suppression of low frequencies, clearly differentiated the EZ from areas of propagation (Grinenko et al., 2018). It has been illustrated that analyzing the fast activity alone is often over-estimated relative to the fingerprint for localization of the EZ (Li et al., 2020). In our case, EZ was limited to the left lingula cortex (mesial to the lesion), and the data was prospectively complemented by the number of predicted EZ electrodes using the "EZ fingerprint" software. In summary, the prospective use of the combined MRI post-processing and MRI-PET data with the "EZ fingerprint" predictive model should be used as a complementary tool in the armamentarium for the presurgical evaluation of "MRI-negative" drug-resistant OLE patients.

Conflict of Interest Statement

The authors declare no conflicts of interest regarding the production of this article. Dr. Gonzalez-Martinez is a consultant for Zimmer-Biomet. Other authors have no personal financial or institutional interest in any of the drugs, materials, or devices described in this article. We confirm that we have read the Journal's position on issues involved in ethical publication and affirm that this report is consistent with those guidelines.

Acknowledgements

The authors are grateful to all the staff members at University of Pittsburgh Medical Center, the patient, and his family for participating in this study.

References

Alves RV, Ribas GEC, Párraga RG, De Oliveira EO. The occipital lobe convexity sulci and gyri: laboratory investigation. J Neurosurg 2012;116:1014–23. https://doi.org/10.3171/2012.1.JNS11978.

Chassoux F, Rodrigo S, Semah F, Beuvon F, Landre E, Devaux B, et al. FDG-PET improves surgical outcome in negative MRI Taylor-type focal cortical dysplasias. Neurology 2010;75:2168–75. https://doi.org/10.1212/WNL.0b013e31820203a9.

Grinenko O, Li J, Mosher JC, Wang IZ, Bulacio JC, Gonzalez-Martinez J, et al. A fingerprint of the epileptogenic zone in human epilepsies. Brain 2018;141:117–31. https://doi.org/10.1093/brain/awx306.

Heo W, Kim JS, Chung CK, Lee SK. Relationship between cortical resection and visual function after occipital lobe epilepsy surgery. J Neurosurg 2018;129:524–32. https://doi.org/10.3171/2017.5.JNS162963.

Huppertz HJ, Grimm C, Fauser S, Kassubek J, Mader I, Hochmuth A, et al. Enhanced visualization of blurred gray-white matter junctions in focal cortical dysplasia by voxel-based 3D MRI analysis. Epilepsy Res 2005;67:35–50. https://doi.org/10.1016/j.eplepsyres.2005.07.009.

Huppertz HJ, Kurthen M, Kassubek J. Voxel-based 3D MRI analysis for the detection of epileptogenic lesions at single subject level. Epilepsia 2009;50:155–6. https://doi.org/10.1111/j.1528-1167.2008.01734.x.

Jian Li, Epileptogenic Zone Fingerprint. https://silencer1127.github.io/software/EZ_Fingerprint/ezf_main (2018). Accessed Jan 2018.

Jobst BC, Williamson PD, Thadani VM, Gilbert KL, Holmes GL, Morse RP, et al. Intractable occipital lobe epilepsy: Clinical characteristics and surgical treatment. Epilepsia 2010;51:2334–7. https://doi.org/10.1111/j.1528-1167.2010.02673.x.

Li J, Grinenko O, Mosher JC, Gonzalez-Martinez J, Leahy RM, Chauvel P. Learning to define an electrical biomarker of the epileptogenic zone. Hum Brain Mapp 2020;41:429–41. https://doi.org/10.1002/hbm.24813.

Thandar Aung *
University of Pittsburgh Comprehensive Epilepsy Center (UPCEC), University of Pittsburgh Medical Center (UPMC), Pittsburgh, PA, USA
* Corresponding author at: University of Pittsburgh Comprehensive Epilepsy Center (UPCEC), 3471 Fifth Avenue, Pittsburgh, PA, 15213.
E-mail address: aung.thandar@outlook.com

Naoki Ikegaya
Department of Neurosurgery, University of Pittsburgh Medical Center, Pittsburgh, PA, USA
Department of Neurosurgery, Graduate School of Medicine, Yokohama City University, Yokohama, Kanagawa, Japan

Lazarus Mayoglou
University of Pittsburgh Comprehensive Epilepsy Center (UPCEC), University of Pittsburgh Medical Center (UPMC), Pittsburgh, PA, USA

Jian Li
Athinoula A. Martinos Center for Biomedical Imaging, Massachusetts General Hospital and Harvard Medical School, Charlestown, MA, USA
Center for Neurotechnology and Neurorecovery, Department of Neurology, Massachusetts General Hospital and Harvard Medical School, Boston, MA, USA

Jorge A. Gonzalez-Martinez
Department of Neurosurgery, University of Pittsburgh Medical Center, Pittsburgh, PA, USA

Accepted 18 August 2023

Available online 1 September 2023